

X-ray analysis of electron Bernstein wave heating in MST

A. H. Seltzman, J. K. Anderson, A. M. DuBois, A. Almagri, and C. B. Forest

Citation: *Rev. Sci. Instrum.* **87**, 11E329 (2016); doi: 10.1063/1.4960161

View online: <http://dx.doi.org/10.1063/1.4960161>

View Table of Contents: <http://aip.scitation.org/toc/rsi/87/11>

Published by the [American Institute of Physics](#)



X-ray analysis of electron Bernstein wave heating in MST

A. H. Seltzman,^{a)} J. K. Anderson, A. M. DuBois, A. Almagri, and C. B. Forest
Department of Physics, University of Wisconsin, Madison, Wisconsin 53706, USA

(Presented 8 June 2016; received 9 June 2016; accepted 8 July 2016;
 published online 22 August 2016)

A pulse height analyzing x-ray tomography system has been developed to detect x-rays from electron Bernstein wave heated electrons in the Madison symmetric torus reversed field pinch (RFP). Cadmium zinc telluride detectors are arranged in a parallel beam array with two orthogonal multi-chord detectors that may be used for tomography. In addition a repositionable 16 channel fan beam camera with a 55° field of view is used to augment data collected with the Hard X-ray array. The chord integrated signals identify target emission from RF heated electrons striking a limiter located 12° toroidally away from the RF injection port. This provides information on heated electron spectrum, transport, and diffusion. RF induced x-ray emission from absorption on harmonic electron cyclotron resonances in low current (<250 kA) RFP discharges has been observed. *Published by AIP Publishing.* [<http://dx.doi.org/10.1063/1.4960161>]

I. MULTI VIEW HARD XRAY SYSTEM

High power RF in tokamaks is routinely diagnosed through free-free bremsstrahlung x-ray emission from RF accelerated electrons on plasma ions.¹ EBW heating location in a spherical tokamak has been observed with pin diode array measuring free-free bremsstrahlung soft x-ray emission.² In our current work on understanding the propagation and absorption of the Electron Bernstein Wave (EBW) in a reversed field pinch plasma, the emission from RF accelerated electrons is quite weak. In order to understand the subtle effects of modest RF power on the RFP plasma, a diagnostic sensitive to small changes in the electron distribution is required. Single photon counting, pulse height analysis, and careful energy filtering are required to isolate the RF enhancement to the x-ray spectrum from background effects.

A multi-chord hard x-ray (HXR) detector system is implemented to measure RF enhancement of x-ray flux. The detector system consists of 14 repositionable single channel CZT detector modules³ that can be placed on “D” and “Q” boxports, with 17 and 11 ports, respectively, displaced 12° toroidally from the RF injection port. The energy resolution of the detectors is particularly important in separating EBW enhanced x-ray flux from the background when injected RF power is much less than ohmic heating. Each detector module is encased in a lead shield and mounted on a cylindrical lead collimator to provide a cylindrical field of view on a chord through the plasma. A 13 mm diameter collimator is mounted on the detector to restrict field of view. The x-ray flux into each detector passes through a 150 μm Be vacuum window which allows photon energies from 4 keV to over 100 keV to be measured. Additional filters of varying material and thickness can be placed

over the x-ray detector to select a specified lower energy cutoff. The detectors are configured on two boxports intersecting at right angles, shown in Figure 1 as “D” and “Q” detector chords, to reconstruct the x-ray emissivity in two dimensions. Emissivity as a simple function of flux surface is not observed.

A 16 channel CZT photon counting HXR camera, shown in Figure 1 as “C” detector chords, with a 55° field of view is located above the RF injection port and provides supplementary information on emissivity at the toroidal angle of the RF antenna. The 16 channel camera has a 200 μm Al filter covering a 3.18 mm pinhole lens and looks through a 120 μm thick Be vacuum window. The aluminum filter thickness was chosen to prevent saturation by attenuating energies below 10 keV, commonly found in the x-ray background when running with auxiliary poloidal current drive which significantly increases plasma pressure and temperature.

II. EBW IN AN RFP

In contrast to a tokamak or stellarator, the region in which an RFP plasma can be heated by externally launched electromagnetic waves is limited to the extreme edge. This is due to the extremely overdense conditions that cuts off O or X modes within a few cm of the edge. Additionally, the magnetic geometry of the RFP does not have a high field side, limiting the options of launch specifics. The EBW has been proposed as a solution for heating and off axis current drive in the RFP due to its ability to propagate past the cutoff into the overdense plasma of high beta fusion experiments. Typical scenarios involve a waveguide antenna launching an X-mode wave from the plasma edge. Due to the density gradient scale length being small compared to the vacuum wavelength of the launched RF, the layers at which electromagnetic cutoff and exclusion of the Bernstein wave are close together, allowing efficient coupling through a narrow evanescent region. In MST plasmas, the EBW propagates inward between 3 and 15 cm, depending on plasma conditions,⁴ and is efficiently damped on

Note: Contributed paper, published as part of the Proceedings of the 21st Topical Conference on High-Temperature Plasma Diagnostics, Madison, Wisconsin, USA, June 2016.

^{a)}Author to whom correspondence should be addressed. Electronic mail: seltzman@wisc.edu.

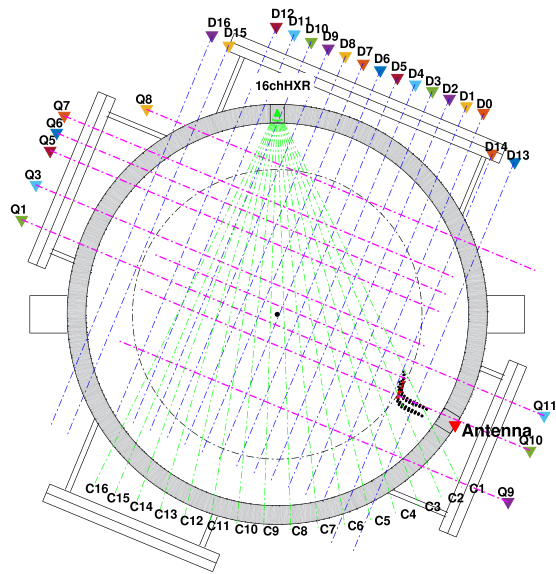


FIG. 1. Configuration of HXR detectors (“D” and “Q” Chords) displaced 12° toroidally from the antenna, and the 16 channel camera (“C” chords) located above the antenna. The black dashed circle is the impact parameter of the RF heating location.

the Doppler-shifted electron cyclotron resonance layer. EBW heated electrons are created in a localized volume and both drift along the field and diffuse radially across it.

III. HXR TARGET EMISSION

The brightest x-ray emission is observed when the high energy electrons strike a limiter on the last closed flux surface (LCFS) approximately 12° toroidally displaced from the injection port. While free-free bremsstrahlung emission is expected for EBW heated electrons, the diagnosis of EBW propagation and deposition is most clear through signatures of enhanced x-rays from target emission. The linear array of HXR detectors views the intersection of the LCFS and a lower hybrid antenna. In Figure 2, RF power measurements are shown in the top half

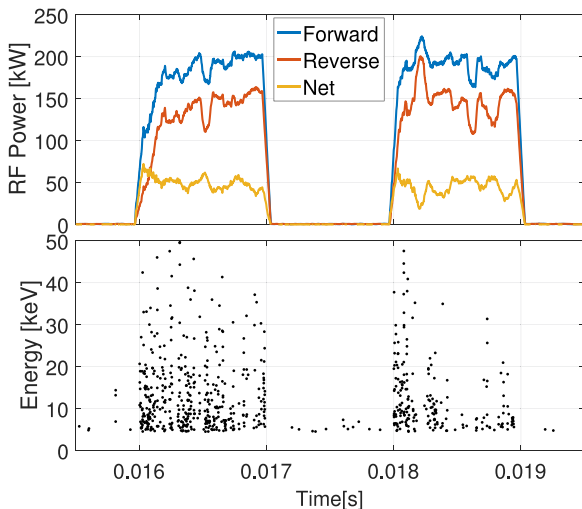


FIG. 2. Forward, reflected, and net RF power injected into plasma (top) correlated with HXR counts (bottom) from chords D0-D5, D13, and D14 during RF injection.

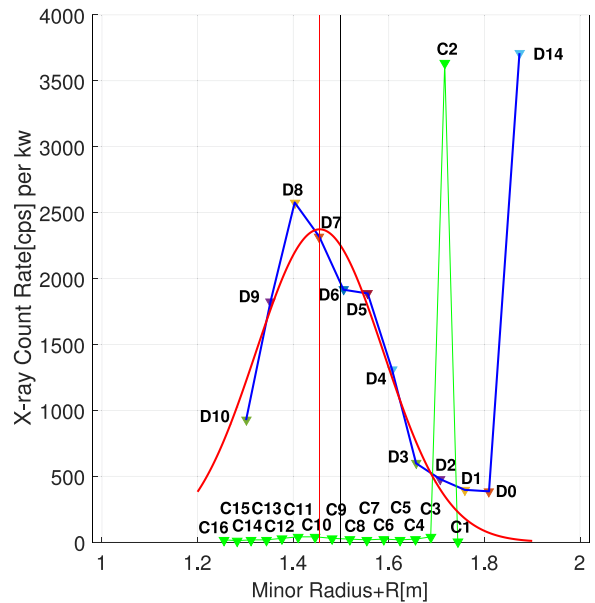


FIG. 3. Measured HXR flux from target emission (“D” chords) and resulting Gaussian fit (red, vertical red line is at peak) of profile at the toroidally displaced target, black line at 1.5 m is machine center. Emission near the RF injection port measured with the 16 channel HXR camera (“C” chords).

of the figure corresponding to ~200 kW of forward power, ~150 kW of reflected power, and ~50 kW of launched power. A significant x-ray flux correlated with RF injection is shown as pulse height analyzed energy counts in the bottom half of Figure 2, with different colors representing counts from different chords. It is noted that in legacy plasmas, the x-ray background is negligible during the RF off periods ($t < 16$ ms, $t = 17-18$ ms, or $t > 19$ ms).

In Figure 3, the average line integrated x-ray flux is plotted versus impact parameter (mapped to an effective major radius crossing at the mid-plane). The individual counts from each chord are averaged together from seven similar EBW-heated discharges and normalized by net input power. The “D” labeled chords are from the direct lines of sight which view the LHCD antenna, and these chords are well fit by a Gaussian. The integrated area is a rough measure of the total RF enhancement in these low background cases. It is observed that the location of the Gaussian center is robustly positioned at the point where the LCFS is nearest to the antenna limiter. Edge emissivity, shown on “D14” is also observed to be high, but is not fitted as part of the target emission. Elevated emission is also observed on the 16 channel HXR camera, chords “C1” and “C2,” located in close proximity to the absorption location of the EBW.

IV. ADVANCED FILTERING STRATEGIES

The RFP can be run with auxiliary pulsed poloidal current drive⁵ (PPCD), which reduces magnetic perturbations, increases confinement, and leads to a dramatically larger background x-ray flux. It presents an interesting target plasma for RF heating due to higher temperatures, steeper gradients, and reduced ohmic input power. For maximum sensitivity to EBW heated electrons, 12.7 mm aperture for the detector is used.

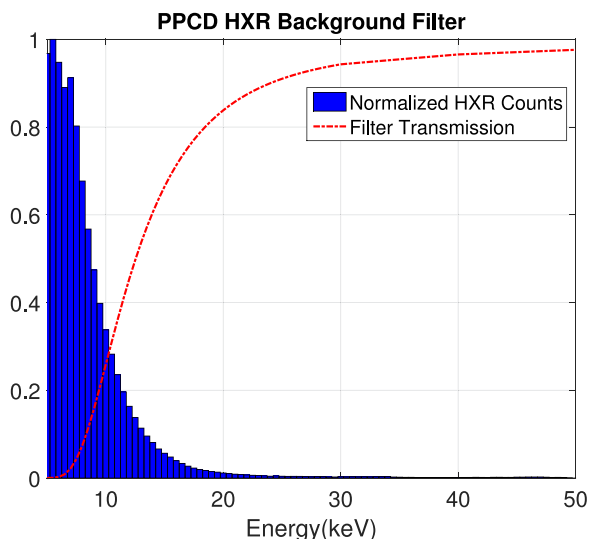


FIG. 4. Measured PPCD background with a $150\ \mu\text{m}$ Be window using restricted apertures showing most emission below 10 keV (histogram) influencing choice of the $150\ \mu\text{m}$ Be + $200\ \mu\text{m}$ Al filter (red dashed line).

In a PPCD plasma the x-ray background increases substantially to the point of saturating the CZT detectors when run with the standard $150\ \mu\text{m}$ Be window. In Fig. 4, the x-ray background is shown in the blue histogram as the normalized number of counts collected during a PPCD plasma without RF injection. It is observed that the majority of the background is below 10 keV in energy. The addition of a $200\ \mu\text{m}$ Al filter may be used to significantly reduce the PPCD background while allowing high sensitivity to the 14-22 keV EBW enhanced x-rays. The transmission of the filter is shown in Fig. 4 as the red dashed line.

X-ray measurements are corrected by the net filter transmission to produce the spectrum from the plasma. Figure 5 shows a comparison between x-ray spectrums with RF heating off (black dash dot line), RF heating on (red solid line), and the difference between the two (green dashed line). The comparison is made by averaging together many similar discharges with a 3 ms injection of RF heating between $t = 16$ and $t = 19$ ms. The “RF off” case is an average of x-ray data later in time ($t = 19$ -22 ms). As the temperature and background fast electron population grow in time throughout the PPCD discharge, the low energy component is greater in the “RF off” case (later in time). The spectrum is monotonically decreasing as normally found in an Ohmically heated plasma. During RF injection (16-19 ms, red line), a very distinct feature is identified in the 14-22 keV energy range as well as a clear increase at energies up to 30 keV. While the RF-induced x-rays are from emission on the LCFS, they prove the existence of RF-accelerated electrons within the plasma. This information is of critical importance when comparing with Fokker-Plank modeling of the wave-plasma interaction—a topic of future work.

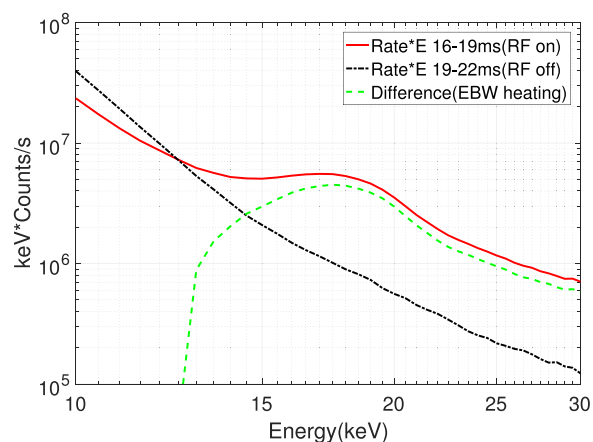


FIG. 5. HXR spectrum corrected for $200\ \mu\text{m}$ Al + $150\ \mu\text{m}$ Be filter during PPCD with RF on and off. $I_p = 248$ kA and $N_e = 0.76 \times 10^{13}/\text{cc}$.

V. CONCLUSIONS

An x-ray diagnostic system to observe EBW based electron heating in the RFP has been implemented. A single photon counting, pulse height analyzing HXR system is used to observe RF heated electrons striking a limiter 12° toroidally away from the RF injection port. During PPCD operation the selection of a $200\ \mu\text{m}$ Al filter is critical in filtering out background flux while maintaining good sensitivity to EBW enhanced x-rays.

SUPPLEMENTARY MATERIAL

See [supplementary material](#) for the digital format of the data shown in this paper.

ACKNOWLEDGMENTS

This material is based on work supported by the U.S. Department of Energy Office of Science, Office of Fusion Energy Sciences program under Award No. DE-FC02-05ER54814.

- ¹S. Von Goeler *et al.*, “Angular distribution of the bremsstrahlung emission during lower hybrid current drive on PLT,” *Nucl. Fusion* **25**(11), 1515 (1985).
- ²S. Shiraiwa *et al.*, “Heating by an electron Bernstein wave in a spherical tokamak plasma via mode conversion,” *Phys. Rev. Lett.* **96**, 185003 (2006).
- ³R. O’Connell, D. J. Den Hartog, and C. B. Forest, “Measurement of fast electron distribution using a flexible, high time resolution hard x-ray spectrometer,” *Rev. Sci. Instrum.* **74**, 2001 (2003).
- ⁴P. K. Chattopadhyay, J. K. Anderson, T. M. Biewer, D. Craig, C. B. Forest, R. W. Harvey, and A. P. Smirnov, “Electron Bernstein wave emission from an overdense reversed field pinch plasma,” *Phys. Plasmas* **9**, 752 (2002).
- ⁵J. M. Reynolds, C. R. Sovinec, and S. C. Prager, “Nonlinear magnetohydrodynamics of pulsed parallel current drive in reversed-field pinches,” *Phys. Plasmas* **15**, 062512 (2008).